Sequential Self-Organization of Silver(I) Layered Materials with Strong SHG by J Aggregation and Intercalation of Organic Nonlinear Optical Chromophores through Mechanochemical Synthesis

Elena Cariati,*,† Roberto Macchi,† Dominique Roberto,† Renato Ugo,† Simona Galli,*,‡ Norberto Masciocchi,‡ and Angelo Sironi§

Dipartimento di Chimica Inorganica, Metallorganica e Analitica and Dipartimento di Chimica Strutturale e Stereochimica Inorganica, Università degli Studi di Milano, Centro di Eccellenza CIMAINA, UdR di Milano dell'INSTM and ISTM-CNR, Via Venezian 21, 20133 Milano, Italy, and Dipartimento di Scienze Chimiche e Ambientali, Università dell'Insubria, Via Valleggio 11, 22100 Como, Italy

Received April 12, 2007. Revised Manuscript Received May 22, 2007

The inorganic−organic hybrid layered material of stoichiometry $[DAMS^+][Ag_5I_6^-]$, characterized by a strong SHG activity, has been prepared mechanochemically by room-temperature ball-milling a mixture of AgI and $[DAMS^+][I^-]$, eventually followed by a moderate heating. By means of electronic absorption spectra, XRPD, and second harmonic generation (SHG) experiments we proved that the intralayer ordering of the $[DAMS^+]$ nonlinear optical chromophores into J-aggregates precedes the interlayer one, on the whole producing, by a sequential process, the "macropolarity" responsible for the strong SHG. The mechanochemical approach was shown to be of general use, as it was successfully applied to the synthesis of the analogous $[DAMS^+][Cu_5I_6^-]$, $[DAZOP^+][Ag_5I_6^-]$, and $[DAES^+][Ag_5I_6^-]$ materials.

Introduction

The search for new materials displaying promising electrical, magnetic, or nonlinear optical (NLO) properties has been recently focused on inorganic−organic hybrid materials.[1] Considerable interest has been given to hybrid materials which show large second-order optical nonlinearity because they properly combine the advantages of the organic NLO chromophores to those of the inorganic network. The second harmonic generation (SHG) of these materials is mainly controlled by the organization, within the crystal lattice, of the organic NLO chromophores, typically characterized by a significant molecular quadratic hyperpolarizability, such as that of stilbazolium-type π-delocalized structures.[2] Such organization has been efficiently pursued following different approaches, for example, by (a) intercalation, as the guest, of cationic organic NLO chromophores within the layers of an anionic, pre-existent, inorganic host, through an ion exchange reaction;[3] (b) spontaneous self-assembly of cationic, organic NLO chromophores and anionic, inorganic motives such as chains[4] and layers;[5] or (c) layer-by-layer deposition, via chemical control[6] or self-assembling,[7] of polar arrays of NLO chromophores on silicon or other substrates. Materials of this kind with appreciable[1d,e] or strong[4,5] SHG are indeed of interest for electrooptical devices.[8]

We have recently described the synthesis and characterization by ab initio X-ray powder diffraction (XRPD) and electronic absorption spectroscopy of the new inorganic−organic material of stoichiometry $[DAMS^+][Cu_5I_6^-]$ (**1**) ($[DAMS^+]$ = *E*-4-(4-dimethylaminostyryl)-1-methylpyridinium; Chart 1), obtained by addition of $[DAMS^+][I^-]$, dissolved in acetonitrile, to a solution of CuI in aqueous KI.[9] Isolation of **1** represents an example of application of

* To whom correspondence should be addressed. E-mail: elena.cariati@unimi.it (E.C.), simona.galli@uninsubria.it (S.G.).

† Dipartimento di Chimica Inorganica, Metallorganica e Analitica, Università degli Studi di Milano.

‡ Università dell'Insubria.

§ Dipartimento di Chimica Strutturale e Stereochimica Inorganica, Università degli Studi di Milano.

(1) (a) Mitzi, D. B. In *Functional Hybrid Materials*; Gomez-Romero, P., Sanchez, C., Ed.; Wiley-VCH Verlag GmbH & Co. KgaA: Weinheim, Germany, 2004; p 347. (b) Rabu, P.; Drillon, M. *Adv. Eng. Mater.* **2003**, *5*, 189. (c) Coe, B. J.; Curati, N. R. *Comments Inorg. Chem.* **2004**, *25*, 147. (d) Kotler, Z.; Hierle, R.; Josse, D.; Zyss, J.; Masse, R. *J. Opt. Soc. Am. B* **1992**, *9*, 534. (e) Horiuchi, N.; Lefaucheux, F.; Ibanez, A.; Josse, D.; Zyss, J. *J. Opt. Soc. Am. B* **2002**, *19*, 1830.

(2) Alain, V.; Blanchard-Desce, M.; Ledoux-Rak, I.; Zyss, J. *Chem. Commun.* **2000**, 353.

(3) (a) See, for example, Coradin, T.; Clément, R.; Lacroix, P. G.; Nakatani, K. *Chem. Mater.* **1996**, *8*, 2153 and references therein. (b) Coradin, T.; Nakatani, K.; Ledoux, I.; Zyss, J.; Clément, R. *J. Mater. Chem.* **1997**, *7*, 853. (c) Makoto, O.; Ishikawa, A. *J. Mater. Chem.* **1998**, *8*, 463.

(4) Guloy, A.; Tang, Z.; Miranda, P.; Srdanov, V. *Adv. Mater.* **2001**, *13*, 833.

(5) Bénard, S.; Yu, P.; Audière, J. P.; Rivière, E.; Clément, R.; Guilhem, J.; Tchertanov, L.; Nakatani, K. *J. Am. Chem. Soc.* **2000**, *122*, 9444.

(6) See, for example, Facchetti, A.; Abbotto, A.; Beverina, L.; van der Boom, M. E.; Dutta, P.; Evmenenko, G.; Pagani, G. A.; Marks, T. J. *Chem. Mater.* **2003**, *15*, 1064. Katz, H. E.; Wilson, W. L.; Scheller, G. *J. Am. Chem. Soc.* **2004**, *116*, 6636 and references therein.

(7) See, for example, Facchetti, A.; Annoni, E.; Beverina, L.; Morone, M.; Peiwang, Z.; Marks, T. J.; Pagani, G. A. *Nat. Mater.* **2004**, *3*, 910 and references therein.

(8) Sanchez, C.; Lebau, B.; Chaput, F.; Boilot, J. P. In *Functional Hybrid Materials*; Gomez-Romero, P., Sanchez, C., Ed.; Wiley-VCH Verlag GmbH & Co. KgaA: Weinheim, Germany, 2004; p 122.

(9) Cariati, E.; Ugo, R.; Cariati, F.; Roberto, D.; Masciocchi, N.; Galli, S.; Sironi, A. *Adv. Mater.* **2001**, *13*, 1665.

10.1021/cm071003e CCC: $37.00
Published on Web 06/30/2007

Chart 1

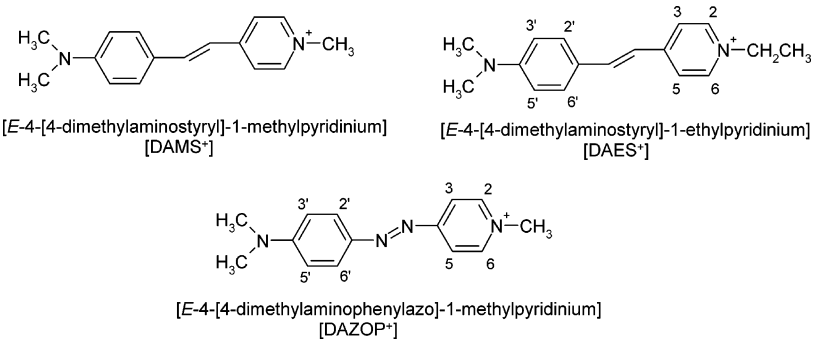

approach b quoted above. One of the major features of this material is certainly its layered structure, where the host inorganic polymeric layers intercalate guest layers of [DAMS$^+$] cations. The organization of the latter, both within the inorganic layers as J-aggregates[10] and through consecutive layers, was considered responsible for the strong SHG activity of **1** (same order of magnitude of [DAMS$^+$][*para*-toluensulfonate$^-$],[11] measured by the Kurtz−Perry method[12] at the nonresonant 1.907 μm incident wavelength). However, upon extending our investigation to the corresponding Ag(I) material, namely, [DAMS$^+$][$Ag_5I_6^-$] (**2**), we were not able to obtain a pure compound, neither by applying the above-mentioned *homogeneous* synthetic method used to prepare **1**[9] nor by a *heterogeneous* alternative (i.e., fractional addition of an acetonitrile solution of [DAMS$^+$][I$^-$] to solid AgI followed by prolonged stirring, see Experimental Section). We thus tried a mechanochemical synthetic approach, which successfully allowed the preparation of **2** and even that of the related materials of stoichiometry [DAZOP$^+$][$Ag_5I_6^-$] (**3**) and [DAES$^+$][$Ag_5I_6^-$] (**4**) ([DAZOP$^+$] = *E*-4-(4-dimethylaminophenylazo)-1-methylpyridinium and [DAES$^+$] = *E*-4-(4-dimethylaminostyryl)-1-ethylpyridinium; Chart 1). Such a mechanochemical synthetic approach not only proved to be advantageous over solution methods but also allowed the characterization of intermediate states. Indeed, the combined use of X-ray powder diffraction (XRPD), electronic absorption spectroscopy (pivotal in confirming the presence of J-aggregates), and SHG measurements (evidencing a significant "macropolarity" within the crystalline lattice) eventually disclosed the sequential mechanism of self-organization of the organic NLO chromophores during the crystal growth. To our knowledge, this kind of self-organization has not been investigated in detail; hereafter, on the basis of converging experimental evidence, a model for this specific crystal growth is proposed.

Experimental Section

Materials and Methods. [DAMS$^+$][I$^-$] and AgI were purchased from Sigma-Aldrich and used as received. Elemental analyses were performed in the Dipartimento di Chimica Inorganica, Metallorganica e Analitica of the Università di Milano. Electronic absorption spectra were recorded on a Jasco V-530 spectrophotometer. ^{1}H NMR were recorded with Bruker AC-200 and Bruker Avance DRX 300 spectrometers. For the numbering used in attributing the ^{1}H NMR signals, see Chart 1.

Synthesis of [DAZOP$^+$][I$^-$]. In a 100 mL beaker, kept in an ice-bath, 4-aminopyridine (1.17 g, 0.012 mol) was dissolved in a mixture of 85% H_3PO_4 (7 mL) and 65% HNO_3 (3 mL); then $NaNO_2$ (0.93 g, 0.013 mol) was added in small portions. Ground ice (12 g) was added, and the solution was stirred for 1 h, after which time a yellow diazole solution was obtained. This solution was then slowly added to *N*,*N*-dimethylaniline (2.8 mL, 0.022 mmol) in a 250 mL beaker kept at a temperature lower than 10 °C. Such solution was added dropwise and under vigorous stirring to a buffer solution prepared by dissolution in water (200 mL) of glacial CH_3-COOH (12.7 mL, 0.222 mol), CH_3COOK (21.3 g, 0.217 mol), and Na_2CO_3 (18.7 g, 0.176 mol) kept at a temperature lower than 10 °C. The resulting orange solid, which separated, was collected by filtration and washed with water until neutrality. The compound was crystallized from water/acetone, filtered, and dried in vacuum; 1.52 g of *N*,*N*-dimethylaniline-4-azopyridine ([DAZOP]) were obtained (yield 58%). [DAZOP$^+$][I$^-$] was obtained by stirring for 3 h at room temperature, in the dark, [DAZOP] (0.500 g, 2.21 mmol) dissolved in CH_2Cl_2 (20 mL) with CH_3I (7.0 mL, 112 mmol). The purple precipitate was filtered and dried in vacuum; 0.71 g of [DAZOP$^+$][I$^-$] were obtained (88% yield). ^{1}H NMR ($CDCl_3$, 25 °C): δ (ppm) 9.05 (AA′BB′, 2H, H_2 and H_6, J = 7.3 Hz), 8.15 (AA′BB′, 2H, H_3 and H_5, J = 7.3 Hz), 7.95 (AA′BB′, 2H, $H_{2'}$ and $H_{6'}$, J = 9.3 Hz), 6.80 (AA′BB′, 2H, $H_{3'}$ and $H_{5'}$, J = 9.3 Hz), 4.6 (s, 3H, H_8), 3.12 (s, 6H, NMe_2). UV−vis in CH_3CN: λ_{max} 549 nm. Anal. Calcd for $C_{14}H_{17}IN_4$: C, 45.66; H, 4.66; N, 15.22. Found: C, 45.74; H, 4.88; N, 14.98.

Synthesis of [DAES$^+$][I$^-$]. CH_3CH_2I (4.8 mL, 59.6 mmol) was added to [*E*-4′-(dimethylamino)-4-stilbazole] (0.191 g, 0.85 mmol) dissolved in CH_2Cl_2 (50 mL). The reaction mixture was stirred at room temperature in the dark for 3 days. The final solution was evaporated under vacuum giving 0.300 g of [DAES$^+$][I$^-$] (93% yield). ^{1}H NMR (CD_3OD, 25 °C): δ (ppm) 8.60 (AA′BB′, 2H, H_2 and H_6, J = 7.3 Hz), 7.98 (AA′BB′, 2H, H_3 and H_5, J = 7.3 Hz), 7.85 (d, 1H, H_7, J = 16.2 Hz), 7.60 (AA′BB′, 2H, $H_{2'}$ and $H_{6'}$, J = 8.9 Hz), 7.1 (d, 1H, H_8, J = 16.2 Hz), 6.80 (AA′BB′, 2H, $H_{3'}$ and $H_{5'}$, J = 8.9 Hz), 4.47 (q, 2H, H_9, J = 7.3 Hz), 3.06 (s, 6H, NMe_2), 1.6 (t, 3H, H_{10}, J = 7.3 Hz). UV−vis in CH_3CN: λ_{max} 472 nm. Anal. Calcd for $C_{17}H_{21}IN_2$: C, 53.70; H, 5.57; N, 7.37. Found: C, 53.67; H, 5.51; N, 7.25.

Mechanochemical Synthesis of [DAMS$^+$][$Cu_5I_6^-$], 1. [DAMS$^+$][I$^-$] (0.039 g, 0.107 mmol) and CuI (0.101 g, 0.532 mmol) were ball-milled in a SPECAMILL mill in an agate vial with three agate balls (0.436 g). The reaction progress was monitored by XRPD. The time required for peaks characterizing **1** to appear depends on both the quantity of reactants and the mill vibration frequency. By diminishing the former or raising the latter, the reaction is complete

(10) Mobius, D. *Adv. Mater.* **1995**, *7*, 437.
(11) Marder, S.; Perry, J. W.; Yakymyshyn, C. P. *Chem. Mater.* **1994**, *6*, 1137.
(12) Kurtz, S. K.; Perry, T. T. *J. Appl. Phys.* **1968**, *39*, 3798.

in less than 30 min. UV−vis in KBr pellets: λ_{max} 510 nm broad, 580 nm narrow. Anal. of the batch obtained by 30 min room-temperature ball-milling followed by 100 min heating at 160 °C. Calcd for $Cu_5C_{16}H_{19}I_6N_2$: C, 14.57; H, 1.45; N, 2.12. Found: C, 12.54; H, 1.47; N, 2.10.

Attempted Homogeneous Synthesis of [DAMS$^+$][Ag$_5$I$_6^-$], 2. [DAMS$^+$][I$^-$] (0.041 g, 0.112 mmol) in CH_3CN (50 mL) was added to AgI (2.11 g; 9.00 mmol) dissolved in aqueous, KI saturated solution. On standing for a few minutes the formation of a red precipitate was observed. The compound was separated by filtration and characterized by elemental analysis, XRPD, and SHG. The former suggested a stoichiometry close to [DAMS$^+$][$Ag_2I_3^-$] (**2***); the X-ray powder diffractograms of the precipitate confirmed the formation of a phase **2*** structurally distinct from **2**, occasionally contaminated by minor amounts of **2**; SHG measurements gave no signal.

Heterogeneous Synthesis of [DAMS$^+$][Ag$_5$I$_6^-$], 2. [DAMS$^+$][I$^-$] (0.039 g, 0.107 mmol) dissolved in CH_3CN (50 mL) was fractionally added to solid AgI (0.126 g, 0.535 mmol). The suspension was stirred at room temperature overnight. After filtration, a dark brown material with metallic luster was obtained as expected for the formation of **2**. However, the purity of different batches of **2** was checked by means of XRPD which always indicated the presence of a minor amounts of a contaminating phase (**2****).

Mechanochemical Synthesis of [DAMS$^+$][Ag$_5$I$_6^-$], 2. [DAMS$^+$][I$^-$] (0.0405 g, 0.111 mmol) and AgI (0.125 g, 0.534 mmol) were ball-milled in a SPECAMILL mill in an agate vial with three agate balls (0.436 g). The reaction progress was monitored by XRPD. The time required for peaks characterizing **2** to appear depends on both the quantity of reactants and the mill vibration frequency. By diminishing the former or raising the latter, the reaction is complete in less than 30 min. UV−vis in KBr pellets: λ_{max} 490 nm broad, 580 nm narrow. Anal. of the batch obtained by 30 min room-temperature ball-milling followed by 100 min heating at 160 °C. Calcd for $C_{16}H_{19}Ag_5I_6N_2$: C, 12.48; H, 1.25; N, 1.82. Found: C, 12.43; H, 1.27; N, 1.85.

Mechanochemical Synthesis of [DAZOP$^+$][Ag$_5$I$_6^-$], 3. [DAZOP$^+$][I$^-$] (0.0405 g, 0.110 mmol) and AgI (0.129 g, 0.550 mmol) were ball-milled for 60 min in a SPECAMILL mill in an agate vial with three agate balls (0.436 g). The dark purple powder thus obtained was then heated at 160 °C for 180 min. UV−vis in KBr pellets: λ_{max} 554 nm broad, 680 nm narrow. Anal. Calcd for $C_{14}H_{17}Ag_5I_6N_4$: C, 10.90; H, 1.11; N, 3.63. Found: C, 11.00; H, 1.17; N, 3.57.

Mechanochemical Synthesis of [DAES$^+$][Ag$_5$I$_6^-$], 4. [DAES$^+$][I$^-$] (0.0416 g, 0.109 mmol) and AgI (0.129 g, 0.550 mmol) were ball-milled for 60 min in a SPECAMILL mill in an agate vial with three agate balls (0.436 g). The dark red powder thus obtained was then heated at 160 °C for 180 min. UV−vis in KBr pellets: λ_{max} 500 nm broad. Anal. Calcd for $C_{17}H_{21}I_6Ag_5N_2$: C, 13.14; H, 1.36; N, 1.80. Found: C, 13.20; H, 1.26; N, 1.75.

Solid-State SHG by Kurtz−Perry[12] Measurements of 2, 3, and 4. The 1064 nm initial wavelength of a Nd:YAG pulsed laser beam was shifted to 1907 nm by stimulated Raman scattering in a high-pressure hydrogen cell. A portion of this beam was directed on sample containing capillaries. The scattered radiation was collected by an elliptical mirror, filtered to select only the second-order contribution and recollected with a Hamamatsu R5108 photomultiplier tube. SHG efficiency was evaluated by taking as reference the SHG signal of [DAMS$^+$][*para*-toluenesulfonate$^-$].[11]

XRPD Analysis of 2, 3 and 4. The powders were gently ground in an agate mortar and then carefully deposited in the hollow of an aluminum sample holder equipped with a quartz zero-background plate (supplied by The Gem Dugout, Swarthmore, PA). To follow the ball-milling experiments, diffraction data were collected with graphite-monochromated Cu Kα radiation, in the 5−35° (2θ) range, on a Philips PW 1800 θ:2θ diffractometer equipped with a Na(Tl)I scintillation detector and a pulse height amplifier discriminator. Generator settings, 40 kV, 40 mA; optics, DS 1°, AS 1°, RS 0.2 mm. In all the other cases, diffraction data were collected with graphite-monochromated Cu Kα radiation, in the 5−105° (2θ) range, on a Bruker AXS D8 θ:θ diffractometer equipped with a Na(Tl)I scintillation detector and a pulse height amplifier discriminator. Generator settings, 40 kV, 40 mA; optics, DS 0.5°, AS 0.5°, RS 0.2 mm. Admitting isomorphism with **1**, a structural refinement was performed on species **2** by the Rietveld method, as implemented in the TOPAS-R suite of programs.[13] The effect of the translational disordered [DAMS$^+$] cations, in the *ab* plane, has been modeled by a single N atom (in 0,0,1/3) with site occupation factor of 3 (corresponding to the total electron count of one [DAMS$^+$] cation per cell) and a large *B* factor (100 Å^2, corresponding to a large vibration of $\langle u^2\rangle^{1/2}$ of about 3.5 Å). Such a model implies a nonzero scattering contribution only for low-angle 00*l* reflections. Final R_p, R_{wp}, R_B, and χ^2 agreement factors, together with details on the data collection and analysis for **2**, can be found in Table 1. Figure 1 shows the final Rietveld refinement plot. Relevant structural parameters can be found in the caption to Figure 4. For **3** and **4**, supposing isomorphism with compounds **1** and **2**, refinements of the cell parameters were performed by the Le Bail method (structureless whole powder pattern fitting), as implemented in TOPAS-R.[13] A synoptic collection of the Le Bail refined lattice parameters of **3** and **4**, with the corresponding figures of merit, can be found in Table 2. Crystallographic data (excluding structure factors) for the reported structure have been deposited with the Cambridge Crystallographic Data Centre (see Supporting Information).

Table 1. Details on the XRPD Data Collection and Analysis of Compound 2[a]

formula	$C_{16}H_{19}Ag_5I_6N_2$
fw, g mol^{-1}	1540.11
system	trigonal
space group	*R*3*m*
a, Å	4.5049(7)
c, Å	38.535(4)
Z	6
V, Å^3	677.3(2)
diffractometer	Bruker AXS D8
T, K	298(2)
F(000)	4092
2θ range, deg	5−105
N_{data}	5001
R_p, R_{wp}	0.119, 0.152
R_B	0.042
χ^2	1.901

[a] $R_p = \sum_i|y_{i,o} - y_{i,c}|/\sum_i|y_{i,o}|$; $R_{wp} = [\sum_i w_i(y_{i,o} - y_{i,c})^2/\sum_i w_i(y_{i,o})^2]^{1/2}$; $R_B = \sum_n||I_{n,o}| - |I_{n,c}||/\sum_i|I_{n,o}|$; $\chi^2 = \sum_i w_i(y_{i,o} - y_{i,c})^2/(N_{obs} - N_{par})$, where $y_{i,o}$ and $y_{i,c}$ are the observed and calculated profile intensities, respectively. The summations were run over *i* data points or *n* independent reflections. Statistical weights w_i are normally taken as $1/y_{i,o}$.

Results and Discussion

The *homogeneous* synthetic method to obtain [DAMS$^+$][$Cu_5I_6^-$] (**1**) consisted of the fractional addition, in large deficiency, of [DAMS$^+$][I$^-$], dissolved in acetonitrile, to CuI, dissolved in aqueous KI.[14]

Unfortunately, because of its low solubility and tendency to grow as dentrites, **1** could not be obtained as single crystals

(13) Topas-R, Bruker AXS: General profile and structure analysis software for powder diffraction data.

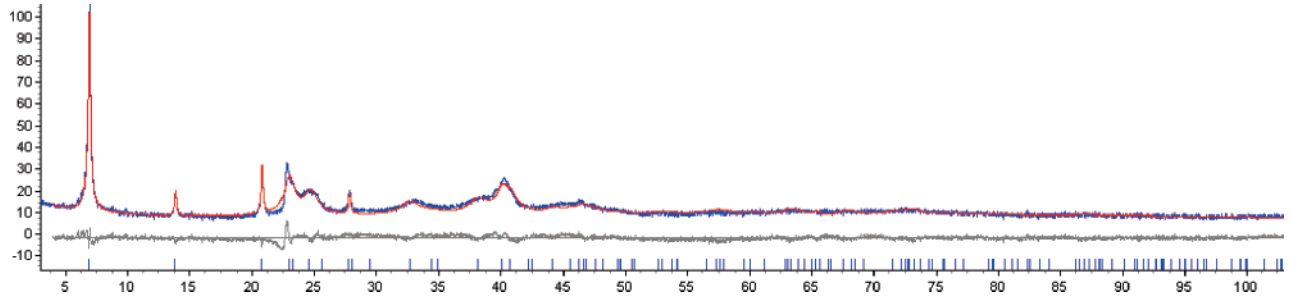

Figure 1. Graphical representation of the Rietveld refinement on species **2** in terms of experimental (blue), calculated (red), and difference (gray) patterns. Peak markers are highlighted at the bottom. Horizontal axis, 2θ (deg); vertical axis, $\sqrt{}$counts.

Table 2. Synoptic Collection of Crystallographic Data and SHG Responses of Materials 2−4[a]

	J	SHG	*a* (Å)	*c* (Å)	*V* (Å^3)	R_{wp}	R_p
2	Y	1	4.5049(7)	38.535(4)	677.3(2)	0.102	0.081
3	Y	0.4	4.493(1)	38.317(7)	669.8(2)	0.126	0.100
4	N	<0.001	4.520(1)	38.683(11)	684.5(4)	0.125	0.098

[a] Presence of J-aggregates, solid-state SHG response against [DAMS$^+$]-[*para*-toluenesulfonate$^-$] at 1097 μm,[11] unit cell parameters and figures of merit from Rietveld (**2**) or Le Bail refinements (**3** and **4**).

suitable for an X-ray structural determination. Therefore, all the retrievable structural information was obtained by ab initio XRPD methods.[9,15] The structural motif of the inorganic part consists of CuI slabs, stacked along the trigonal axis, formed by two parallel, slightly corrugated sheets. The presence of some organization of the [DAMS$^+$] chromophores into J-aggregates was inferred by the electronic absorption spectrum, showing the typical narrow band,[10] red-shifted (580 nm) with respect to that of [DAMS$^+$] in solution (471 nm).[9]

Extending our investigation to the corresponding Ag(I) material, we observed that a *homogeneous* synthetic procedure, analogous to that followed to obtain **1**, invariably led to the formation of an undesired material, **2*** (see Experimental Section). The XRPD pattern showed that **2*** was isomorphous neither to **1** nor to the salt [DAMS$^+$]$_2$[$Cu_2I_4^{2-}$].[15] Moreover, it also revealed that, occasionally, variable amounts of [DAMS$^+$][$Ag_5I_6^-$] (**2**) were present as a minor phase. Because **2*** proved to be SHG inactive, it was not the subject of further investigations. Even an alternative *heterogeneous* synthetic method, consisting of the fractional addition of [DAMS$^+$][I$^-$], dissolved in acetonitrile, to solid AgI followed by prolonged stirring, was not completely successful, the layered material **2** being invariably contaminated by another, not characterized, side product, **2****. Prompted by these unsatisfactory results and by the recent publications on efficient mechanochemical methods for the synthesis of organic[16] and metal-coordination compounds,[17] we attempted the mechanochemical synthesis of **2**.

Prolonged ball-milling of [DAMS$^+$][I$^-$] with 5 molar equiv of AgI at room-temperature yield a dark brown material with metallic luster, corresponding to the expected [DAMS$^+$]-[$Ag_5I_6^-$] stoichiometry and showing an XRPD trace similar to that of **1**, that is, confirming the formation of the analogous layered compound **2**. As a matter of fact such a mechanochemical approach proved to be of broader use, because also the corresponding Cu(I) material **1** was easily obtained by applying this method.

The mechanochemical synthesis of **2** was then monitored by a step-by-step approach, by simultaneously coupling XRPD (Figure 2), SHG (by the Kurtz−Perry method),[12] and electronic absorption spectroscopy (Figure 3) observations. After ball-milling for 240 min, although the XRPD peaks of both reactants are still clearly visible, the typical 00*l* ones of the layered structure of **2** are already detectable (Figure 2c), without the occurrence of peaks corresponding to contaminating materials such as **2*** or **2****. Successive mechanical treatment, up to 540 min, leads to further consumption of reactants, *but the broader* 00*l peaks of* **2** indicate *its concomitant loss of crystallinity* (Figure 2d,e).

The easy formation of **2** by mechanical treatment, at room temperature, of high-melting reactants (AgI, mp 550 °C, and [DAMS$^+$][I$^-$], mp 280 °C) is difficult to explain exclusively on the basis of localized micro-meltings promoted by the mechanical work, as *local* temperatures inside ball mills do not exceed 110 °C.[16a] Thus, a true solid−solid reaction appears to be plausible. As proposed by Balema et al.,[16a] mechanical treatment probably enables easy solid state

(14) By increasing the amount of [DAMS$^+$][I$^-$] added to the aqueous solution of CuI in KI, the centrosymmetric, NLO-inactive, [DAMS$^+$]$_2$-[$Cu_2I_4^{2-}$] salt, containing the [$Cu_2I_4^{2-}$] dimer, precipitates in the form of single crystals. Anal. Calcd for $Cu_2C_{20}H_{38}N_4I_4$: C, 21.56; H, 3.45; N, 5.03. Found: C, 21.52; H, 3.48; N, 5.05. Crystal data: $C_{32}H_{38}N_4$-Cu_2I_4, fw = 1113.39 g mol^{-1}; triclinic, $P\bar{1}$, a = 8.646(1), b = 9.443(2), c = 11.988(2) Å; α = 74.06(1), β = 80.12(1), γ = 76.59(1)°; V = 909.3(3) Å^3; Z = 2; ρ_{calcd} = 2.033 g cm^{-3}; F(000) = 528; μ(Mo Kα) = 4.59 cm^{-1}. Data were collected on an Enraf Nonius CAD4 automated diffractometer. There were a total of 3184 acquired (and unique) reflections in the $6 < 2\theta < 49.9°$ range. R(F), wR(F^2), and GOF were 0.028, 0.071, and 1.073 respectively, for 2662 observed [$I > 2\sigma(I)$] reflections, 189 parameters, and 7 restraints. The highest peak and deepest hole were 0.37 and −0.62 e Å^{-3}. Crystallographic data (excluding structure factors) are deposited with the Cambridge Crystallographic Data Centre as No. CCDC 642781.

(15) Masciocchi, N.; Galli, S.; Sironi A. *Comm. Inorg. Chem.* **2005**, *26*, 1 and references therein.

(16) See, for example, (a) Balema, V. P.; Wiench, J. W.; Pruski, M.; Pecharsky, V. K. *Chem. Commun.* **2002**, 724. (b) Kaupp, G. *Cryst. Eng. Commun.* **2003**, *5*, 117.

(17) See, for example, (a) Balema, V. P.; Wiench, J. W.; Pruski, M.; Pecharsky, V. K. *J. Am. Chem. Soc.* **2002**, *124*, 6245. (b) Braga, D.; Grepioni, F. *Chem. Commun.* **2005**, 3635.

(18) (a) Borisova, A. P.; Petrova, L. A.; Makhaev, V. D. *Zh. Obshch. Khim.* **1992**, *62*, 15. (b) Makhaev, V. D.; Borisova, A. P.; Petrova, L. A.; Karpova, T. P. *Russ. J. Inorg. Chem.* **1996**, *41*, 394. (c) Makhaev, V. D.; Borisova, A. P.; Petrova, L. A. J. *Organomet. Chem.* **1999**, *590*, 222. (d) Mostafa, M. M.; Gomaa, E. A. H.; Mostafa, M. A.; El-Dossouki, F. I. *Spectrochim. Acta A* **1999**, *55*, 2869. (e) Orsa, D.; Ho, D. M.; Takacs L.; Mandal, S. K. *Abstr. Pap.−Am. Chem. Soc.* **2000**, 220. (f) Nichols, P. J.; Raston, C. L.; Steed, J. W. *Chem. Commun.* **2001**, 1062. (g) Paneque, A.; Fernandez-Bertran, J.; Reguera, E.; Yee-Madeira, H. *Transition Met. Chem.* **2001**, *25*, 76.

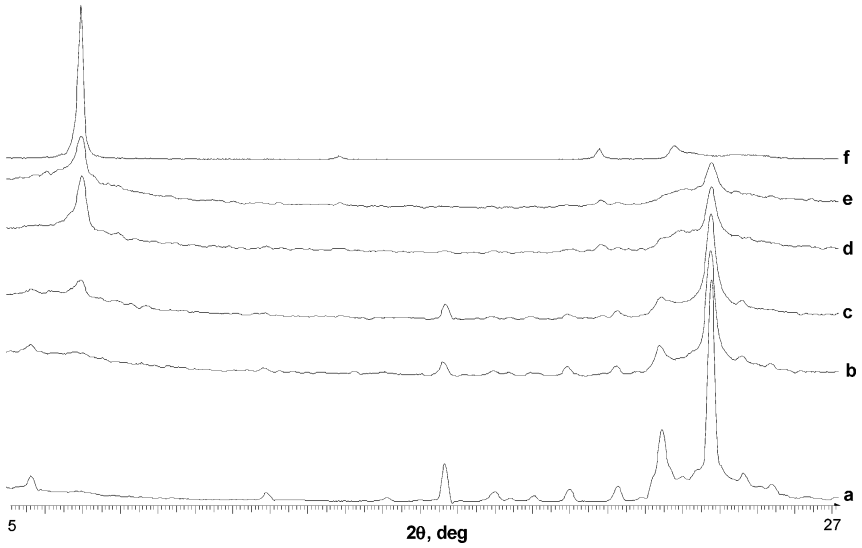

Figure 2. XRPD monitoring of a 5:1 mixture of AgI and [DAMS$^+$][I$^-$] (a) as prepared; (b−e) after 150, 240, 420, and 540 min with room-temperature ball-milling, respectively, and (f) after 30 min with room-temperature ball-milling followed by 100 min heating at 160 °C. Horizontal axis, 2θ (deg).

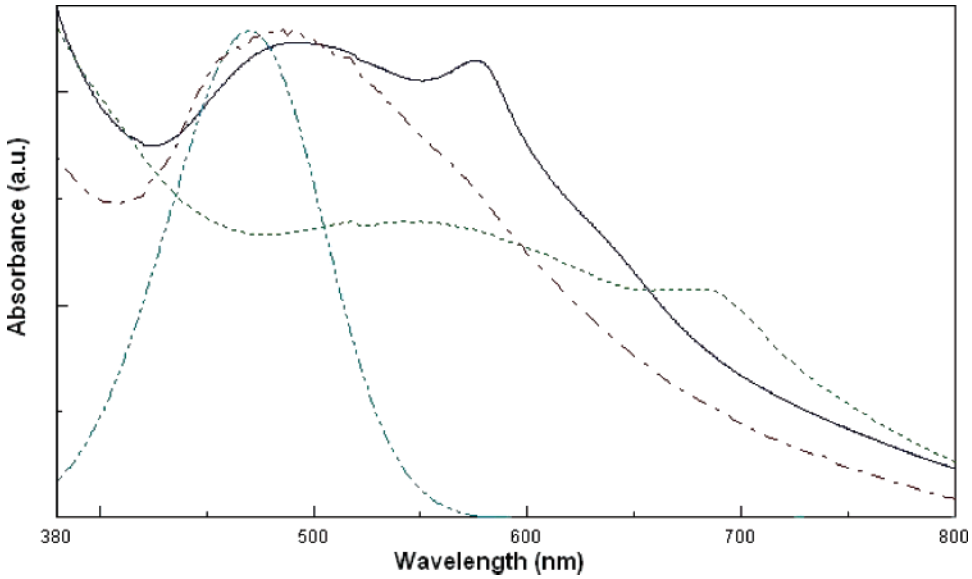

Figure 3. Electronic absorption spectra in KBr of (a) **2** after 540 min of room-temperature ball-milling (solid line), (b) **3** after 60 min of ball-milling and successive 180 min of heating at 160 °C (dotted line), (c) **4** after 60 min of ball-milling and successive 180 min of heating at 160 °C (dashed−dotted line), and (d) [DAMS$^+$][I$^-$] in CH_3CN (dashedEnDash−dotted−dotted line). The spectra of **2** after 240 and 420 min of room-temperature ball-milling are visually similar to that in a.

interactions between the reactants by (i) breaking their crystallinity and (ii) providing the energy for their mass transfer. Actually, we have observed that, in the same conditions (reactants quantity and milling period), uninterrupted milling leads to a less advanced reaction than applying periodic manual stirring. The *intimate* contact between reactants (promoting mass transfer), which is reinforced by stirring but not by continuous milling (favoring agglomeration), is thus more relevant than local heating. As a further confirmation, neither mere contact between the reactants, nor mixing in a mortar, nor heating at 110 °C without stirring promotes steps i and ii.

Unlike other cases, the recovery of **2** does not require, to accomplish the reaction, a subsequent workup, such as heating or dissolution in appropriate solvents.[18] These two-step procedures do not provide a definitive evidence that the complete reaction takes place during the mechanical processing and not because of the subsequent treatment. For instance, this latter event was, for example, shown to be pivotal in the solid-state synthesis of chromium acetylacetonate, which does not form during ball-milling of a mixture of solid $CrCl_3$ and $NaO_2C_5H_7$, yet is obtained only after heating in vacuum the mechanically treated mixture of reactants.[18b]

The batches of **2** obtained by a series of consecutive milling steps at room temperature (240, 420, and 540 min) are characterized not only by a modest crystallinity (Figure 2) but also by slightly different yet *poor* SHG activities (less than 0.1% that of [DAMS$^+$][*para*-toluenesulfonate$^-$][11]).

(19) Yi, T.; Clément, R.; Haut, C.; Catala, L.; Gacoin, T.; Tancrez, N.; Ledoux, I.; Zyss, J. *Adv. Mater.* **2005**, *17*, 335.

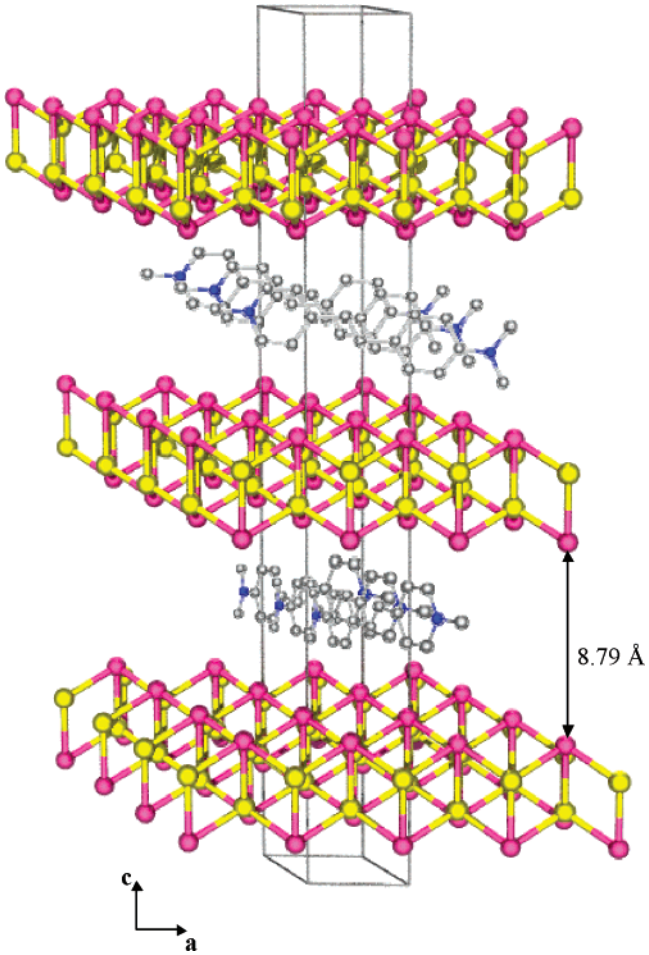

Figure 4. Schematic representation of the wavy two-dimensional slabs of the AgI host lattice, stacked parallel to *c* [I in 0,0,0.1141(1); Ag in 0,0,0.1891(2); Ag−I 2.862(4) Å (3×) and 2.89(1) Å (1×)]. The (diffraction invisible) organic [DAMS$^+$] cations have been inserted within the inorganic layers according to the suggestion discussed in the text (see also refs 21 and 22). At a pictorial drawing level, the figure can be considered representative also of the Cu analogue **1**.

Amazingly, the self-organization of the [DAMS$^+$] chromophores into J-aggregates, usually responsible for a very large SHG,[3,19] has already taken place after the first milling step, as indicated by the typical narrow and red-shifted band, centered at 580 nm, detectable in the electronic absorption spectrum (Figure 3). Incidentally, as observed for **1**,[9] when **2** is dissolved in acetonitrile, the absorption spectrum becomes identical to that of [DAMS$^+$][I$^-$] in the same solvent (Figure 3), with an absorption band at 471 nm, confirming the expected disruption of [DAMS$^+$] J-aggregates by dissolution of **2** in a polar organic solvent.

Trying to increase the crystallinity of **2**, we annealed a 30 min milled sample at 160 °C for 100 min. The better quality of the XRPD trace of the annealed product (Figure 2f) and its strongly improved SHG, of the same order of magnitude of **1** (Table 1), suggest both a better degree of crystallinity and a larger "macropolarity" within the crystal network. Assuming annealed **2** to be isostructural to **1**, a Rietveld refinement was performed (see Experimental Section). Figure 1 graphically shows the match between the experimental, calculated, and differenced patterns, while relevant structural parameters are gathered in the caption to Figure 4. As for **1**, even in the case of **2** we can describe the inorganic host as consisting of polymeric AgI double layers stacked along the trigonal axis, with an interslab spacing of *c*/3 (Figure 5); it is worth noting that X-ray diffraction gives information just on the host. As calculated by SMILE,[20] the intraslab empty volume, per slab, per unit cell, is 104 Å^3. Thus, the guest [DAMS$^+$], longer than the *a* and *b* axes (estimated volume 262 Å^3, estimated length 17 Å), must extend over three adjacent unit cells. Therefore, it is not subject to any translational or point symmetry operator of the host lattice and does contribute just to the low angle 00*l* Bragg reflections.

According to the above-reported experimental observations, we can deduce that, within two host inorganic layers, the [DAMS$^+$] guests are (i) "edge-on", but slightly tilted with respect to the *c* axis;[21] (ii) with iso-oriented dipoles (as witnessed by the very high SHG); (iii) densely packed (as J-aggregates); but (iv) translationally disordered. Note that the presence of an *average* centrosymmetric host lattice does not contrast with the observed SHG activity. Indeed, it has been already reported that [DAMS$^+$] and other stilbazolium-like NLO chromophores give rise, upon intercalation into the centrosymmetric MPS_3 lattice,[3a] to SHG active materials through the formation of J-aggregates.

Noteworthy is that electronic absorption spectroscopy, SHG, and XRPD measurements can provide distinct pieces of information about the step-by-step process of self-organization of the [DAMS$^+$] NLO chromophores within the crystal structure of **2**. XRPD only detects the [$Ag_5I_6^-$] host layered structure, while electronic absorption spectroscopy proves the intralayer [DAMS$^+$] guest organization (by J aggregation). Finally, SHG, requiring a "macroscopic" polarity within the crystal lattice, is sensitive to both intra- and interlayer guest ordering. For instance, formation of **1** was explained to occur by a selective self-recognition process between host and guests.[9] The present consecutive milling experiments add further evidence, suggesting a sequential process: indeed, the electronic spectra show that intralayer guests ordering into J-aggregates takes place rather easily, while the concomitant poor SHG responses suggest that guest organization over adjacent layers within the crystal structure is not merely accomplished upon mechanical treatment (promoting defect formation) yet requires thermal annealing (favoring defect elimination). Thus, the "macroscopic" polarity is produced only at a later stage, by thermal induction.

Stimulated by these findings, we applied the same mechanochemical synthetic method to the related NLO chro-

(20) Eufri, D.; Sironi, A. *J. Mol. Graphics* **1989**, *7*, 165.

(21) The interslab translation in species **2** is 12.84 Å (*c*/3). Nevertheless, to draw a more realistic picture of the [DAMS$^+$] cations packing within the slabs, the van der Waals radii of the atoms reasonably involved in the layer···[DAMS$^+$]···layer interactions must be taken into consideration. Considering the negative charges mainly localized on the iodine atoms and the positive ones on the methylated heterocyclic nitrogen atoms, I(δ^-)···(δ^+)H−C−N−C−H(δ^+)···(δ^-)I interactions would develop between adjacent layers. The shortest I···I interlayer distance is 8.79 Å (Figure 4), while the expected length of the I(δ^-)···(δ^+)H−C−N−C−H(δ^+)···(δ^-)I "moiety" is ca. 10.3 Å. This would imply some tilting of the [DAMS$^+$] cations with respect to the *c* axis; however, it must be pointed out that the I(δ^-)···(δ^+)H−C−N−C−H(δ^+)···(δ^-)I interactions possess a certain degree of electrostactic character, so distances computed from van der Waals radii are somewhat overestimated.

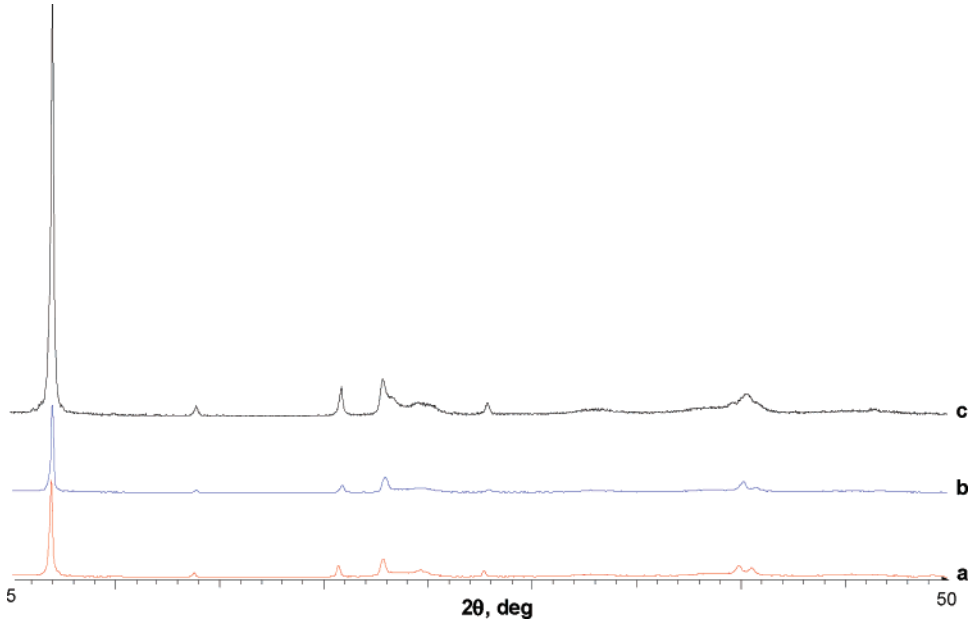

Figure 5. X-ray powder diffractogram of (a) [DAES$^+$][$Ag_5I_6^-$], **4**, (b) [DAZOP$^+$][$Ag_5I_6^-$], **3**, and (c) [DAMS$^+$][$Ag_5I_6^-$], **2**, obtained by ball-milling plus heating. Horizontal axis, 2θ (deg).

mophores [DAZOP$^+$] and [DAES$^+$] (Chart 1), that is, modifying, with respect to [DAMS$^+$], either the bridge between the rings or the substituent on the heterocyclic nitrogen atom. In both cases, after 60 min ball-milling followed by 180 min heating at 160 °C, the formation of the expected layered compounds [DAZOP$^+$][$Ag_5I_6^-$] (**3**) and [DAES$^+$][$Ag_5I_6^-$] (**4**) was confirmed by XRPD (Figure 5) and by analytical evidence (see Experimental Section). While the electronic absorption spectrum of **3** displayed the peculiar narrow band typical of J-aggregates (centered at 680 nm), the same did not occur for **4** (Figure 3). In agreement with such evidence, while **3** showed a significant SHG activity (even though lower than that of **2**), **4** proved to be a rather poor SHG material (Table 2).

The SHG response of these layered structures can be traced back to distinct contributions. First is the presence of J aggregation. Indeed, the low SHG of **4** can be related to the substitution of a methyl with an ethyl group, shifting from [DAMS$^+$] to [DAES$^+$], which hampers a close approach of nearby chromophores into J-aggregates, as confirmed by its electronic absorption spectrum. However, their cofacial disposition and head-to-tail alignment remain substantially unaffected, still allowing the rhombohedral ordering of the host layers, as confirmed by Le Bail refinements successfully performed on the XRPD patterns of **3** and **4** (Figure 5), assuming an $R\bar{3}m$ lattice, as for **1**. The results (cell parameters and figures of merit) are gathered in Table 2. The second aspect affecting the SHG activity is the formation of helical domains of guests within consecutive layers, leading to a "macroscopic" polarity along the *c* axis.[22] Actually, in spite of sharing the very same crystalline framework (of the host!), materials **2**, **3**, and **4** show different SHG efficiencies. Thus, this can be due to a different degree of errors in the interlayer order (of the guests!).

(22) Alternatively, the consecutive guest layers could be iso-oriented (leading to a "macroscopic" polarity lying in the *ab* plane). We do not have any direct evidence to discriminate between the two hypotheses; however, the presence of equally oriented guest layers should promote some (*yet unobserved*) distortion of the rhombohedral host lattice. Therefore, we propose the hypothesis of the helical domains.

Conclusions

We have here reported the first mechanochemical synthesis of layered hybrid inorganic−organic materials displaying strong SHG activity. We have also demonstrated that the combined use of XRPD (capable of disclosing the structural details of this class of compounds), electronic absorption spectroscopy (pivotal in confirming the presence of J-aggregates), and SHG measurements (highlighting the significant "macropolarity" within the crystalline lattice) proves the sequential mechanism of self-organization of the organic NLO chromophores during the crystal growth: first (and easily) the intralayer NLO chromophores order, within the inorganic layers, into J-aggregates; subsequently, upon heating, a partial interlayer ordering along the *c* axis occurs, promoting the manifestation of a "macroscopic" polarity. These results confirm our previous suggestion:[9] the localized charge of [DAMS$^+$] enforces spontaneous poling within one guest layer and imparts a definite "order" to the host Cu(I) vacancies, eventually determining the orientation of the nearby guest layer, that is, the building up of a "macroscopic" ordering, the origin of the very high SHG response.

Noteworthy is such step-by-step spontaneous building of a layered macroscopic polarity having some similarity with the layer-by-layer self-assembly of polar arrays of NLO chromophores.[7]

Notably, the structural features of the guest organic cations within the periodic host inorganic lattice could not be directly inferred by our XRPD measurements, because the disordered moieties do not significantly contribute to Bragg peak

intensity. Accordingly, the packing environment of these "invisible" molecules could only be assessed by their spectral features.

Acknowledgment. This work was supported by MIUR (FISR 2001, FIRB 2003, PRIN 2005) and Fondazione CARIPLO (2005). S.G. and N.M. thank the Fondazione Provinciale Comasca for funding.

Supporting Information Available: Crystallographic information (CIF). This material is available free of charge via the Internet at http://pubs.acs.org. Copies of the data (No. CCDC 642780) can also be obtained free of charge upon application to CCDC, 12 Union Road, Cambridge CB2 1EZ, U.K. (fax, (+44)1223 336-033; e-mail, deposit@ccdc.cam.ac.uk).

CM071003E